Alanine-Scanning Mutagenesis in the Signature Disulfide Loop of the Glycine Receptor α1 Subunit: Critical Residues for Activation and Modulation

Claude M. Schofield,*[,‡,||] James R. Trudell,[⊥] and Neil L. Harrison[§,||]

Graduate Program in Neuroscience, Departments of Anesthesiology and Pharmacology, Weill Medical College of Cornell University, New York, New York 10021, and Department of Anesthesiology, Beckman Program for Molecular and Genetic Medicine, Stanford University, Stanford, California 94305-5117

Received December 1, 2003; Revised Manuscript Received June 2, 2004

ABSTRACT: The glycine receptor enables the generation of inhibitory postsynaptic currents at synapses via neurotransmitter-dependent activation. These receptors belong to the ligand-gated ion channel gene superfamily, in which all members are comprised of five subunits, each of which possesses a signature 13-residue disulfide loop (Cys loop) in the extracellular domain. In this study, we used alanine-scanning mutagenesis of the residues between C138 and C152 of the Cys loop of the glycine receptor α1 subunit to identify residues critical for receptor activation and allosteric modulation. Mutation of L142, F145, or P146 to alanine produced decreases in the potency, maximal amplitude, and Hill coefficient for currents elicited by glycine and impaired receptor activation by the agonist taurine. These residues, along with D148, are positionally conserved in the family of LGIC subunits. Mutation at several other positions had little or no effect. The inhaled anesthetics halothane and isoflurane potentiate submaximal agonist responses at wild-type receptors, via an allosteric site. The mutations L142A, F145A, P146A, and D148A abolished positive modulation by these anesthetics, in some cases revealing a small inhibitory effect. A molecular model of the glycine receptor α1 subunit suggests that the Cys loop is positioned in a region of the receptor at the interface between the extracellular and transmembrane domains and that the critical functional residues identified here lie along the face of a predominantly hydrophobic surface. The present data implicate the Cys loop as an important functional moiety in the process of glycine receptor activation and allosteric regulation by anesthetics.

The ligand-gated ion channel (LGIC)[1] family includes the glycine (GlyR), γ-aminobutyric acid type-A ($GABA_A$), 5-hydroxytryptamine type-3 ($5\text{-}HT_3$), and nicotinic acetylcholine (nACh) receptors. These channels are pentameric proteins that are clustered at the postsynaptic membrane where they subserve fast chemical neurotransmission (*1*). LGIC member subunits share significant sequence homology and consist of a large, extracellular ligand-binding domain made up largely of β sheets (*2*), four transmembrane α-helical segments (*3*), and an intracellular component of unknown structure. Numerous studies have identified amino acid residues critical for LGIC assembly, agonist affinity, and conductance (*4*, *5*, *6*). Less well described are the structural domains involved in the conformational changes required for the coupling of ligand binding to channel gating.

The GlyR is an attractive LGIC for study, because of its structural simplicity; a functional receptor can be assembled in vitro as a homomer of five α subunits. In addition, the receptor has physiologic significance in mediating inhibition in the spinal cord and brain stem (reviewed in refs *7* and *8*). Allosteric modulation of the GlyR presents a novel therapeutic approach at inhibitory synapses (*9*), as well as a potential mechanism for the actions of some anesthetics (*10*). The inhaled general anesthetics halothane and isoflurane enhance glycine receptor sensitivity to agonist (*11*), a process termed potentiation. Site-directed mutagenesis studies in the GlyR α1 subunit (*12*) suggested the existence of a cavity located between adjacent transmembrane helices (*13*) within which volatile anesthetics might bind (*14*). However, the molecular mechanism by which volatile anesthetics enhance receptor activation by agonist remains unknown.

Recent studies of the $GABA_A$ and glycine receptors have implicated an aspartic acid residue within the signature disulfide loop (Cys loop) of the extracellular domain as a potential mediator of the gating process (*15*, *16*, *17*). This residue is highly conserved in all LGIC member subunits and has been proposed to reside at a region between hydrophobic and hydrophilic domains of the receptor (*18*). The presence of additional conserved residues within the Cys loop in the LGIC superfamily might imply that this common structural feature plays a significant role in receptor function. In the present study, we used site-directed mutagenesis, functional expression, and molecular modeling to investigate the functional role of the amino acids within the Cys loop of the GlyR α1 subunit. We found that several of the most

* To whom correspondence should be addressed: C. V. Starr Laboratory for Molecular Neuropharmacology, Department of Anesthesiology, Room A1040, Weill Medical College of Cornell University, 525 East 68th Street, New York, NY 10021. Phone: 212-746-1150. Fax: 212-746-4879. E-mail: cms2002@med.cornell.edu.

‡ Graduate Program in Neuroscience.

§ Departments of Anesthesiology and Pharmacology.

|| Weill Medical College of Cornell University.

⊥ Stanford University.

[1] Abbreviations: GlyR, glycine receptor; LGIC, ligand-gated ion channel; TM, transmembrane segment; $GABA_A$, γ-aminobutyric acid type-A receptor; HEK, human embryonic kidney; AChBP, acetylcholine-binding protein.

10.1021/bi036159g CCC: $27.50
Published on Web 07/13/2004

highly conserved residues appear to be important for receptor activation and noted that these Cys loop residues also influence allosteric modulation of the GlyR by inhaled anesthetics.

MATERIALS AND METHODS

Mutagenesis and Expression. The cDNA encoding the human GlyR α1 (hGlyRα1) subunit was subcloned into the pCIS2 expression vector. Site-directed mutagenesis was performed using the QuikChange method (Stratagene, La Jolla, CA). All mutant clones were confirmed through automated fluorescent DNA sequencing (Rockefeller University, NY). Wild-type or mutant receptor cDNA was transiently expressed in human embryonic kidney (HEK) 293 cells (American Type Culture Collection, Rockville, MD) cultured in Eagle's minimal essential medium (Sigma Chemical, St. Louis, MO) supplemented with 5% fetal bovine serum (Hyclone, Logan, UT), L-glutamine (0.292 μg/mL; GIBCO BRL, Grand Island, NY) and penicillin−streptomycin (100 units/mL; 100 μg/mL, GIBCO). For electrophysiological recordings, cells were plated onto glass coverslips coated with poly-D-lysine (Sigma). Coverslips of HEK 293 cells were transfected with 2.5 μg of each cDNA plasmid using the calcium phosphate precipitation method. Cells were washed after 24 h of contact with cDNA precipitate and used for patch-clamp recording at 48−72 h post transfection.

Electrophysiology. Glycine- and taurine-gated chloride currents were recorded at room temperature using the whole-cell patch-clamp method. Cover slips of transfected HEK 293 cells were transferred to a large chamber (60 mL) and perfused continuously at a flow rate of 1.1 mL/min with extracellular solution (145 mM NaCl, 3 mM KCl, 1.5 mM $CaCl_2$, 1 mM $MgCl_2$, 6 mM D-glucose, and 10 mM HEPES/NaOH (adjusted to pH 7.4). Whole-cell patch-clamp recordings from HEK 293 cells (voltage clamped at −60 mV) were made using the Axopatch 1C amplifier (Axon Instruments, Foster City, CA). Patch pipets were at a resistance of 4−5 MΩ and contained 145 mM *N*-methyl-D-glucamine hydrochloride, 5 mM dipotassium ATP, 1.1 mM EGTA, 2 mM $MgCl_2$, 5 mM HEPES/KOH, and 0.1 mM $CaCl_2$ (pH 7.2). Taurine or glycine and halothane or isoflurane were applied rapidly (~50 ms exchange time) to the cell by local perfusion using a motor-driven solution exchange device (Rapid Solution Changer RSC-100; Molecular Kinetics, Pullman, WA). Laminar flow was maintained via a multichannel infusion pump (WPI, Sarasota, FL). The solution changer was driven by protocols in the acquisition program of pCLAMP 5 (Axon). Responses were low-pass-filtered and digitized with the TL-1−125 interface (Axon) and stored for off-line analysis.

Data Analysis and Statistics. The peak current amplitude of each glycine response was measured for each cell, and the agonist concentration−response amplitude data were fitted using a sum of the least-squares method to a Hill equation of the following form:

$$I = I_{max}[\text{agonist}]^{n_H}/([\text{agonist}]^{n_H} + EC_{50}{}^{n_H})$$

where I is the peak current, I_{max} is the maximum current amplitude, [agonist] is the agonist concentration, EC_{50} is the agonist concentration eliciting a half-maximal current, and n_H is the Hill coefficient. The relative efficacy (ϵ) of taurine is defined as $\epsilon = I_{max(Tau)}/I_{max(Gly)}$, where $I_{max(Tau)}$ is the maximal current elicited by a saturating concentration of taurine and $I_{max(Gly)}$ is the maximal current elicited by a saturating concentration of glycine. Statistical significance was assessed using a one-way ANOVA with a Dunnett's multiple comparison post test. Data are presented as mean ± SE, with n = number of cells tested.

Gly α1	^{138}**C**	P	M	D	**L**	K	N	**F**	**P**	M	**D**	V	Q	T	**C**^{152}
Gly α2	^{145}**C**	P	M	D	**L**	K	N	**F**	**P**	M	**D**	V	Q	T	**C**^{159}
Gly α3	^{138}**C**	P	M	D	**L**	K	N	**F**	**P**	M	**D**	V	Q	T	**C**^{152}
Gly β	^{161}**C**	P	L	D	**L**	T	L	**F**	**P**	M	**D**	T	Q	R	**C**^{175}
$GABA_A$ α1	^{139}**C**	P	M	H	**L**	E	D	**F**	**P**	M	**D**	A	H	A	**C**^{153}
$GABA_A$ β2	^{136}**C**	M	M	D	**L**	R	R	**Y**	**P**	L	**D**	E	Q	N	**C**^{150}
$GABA_A$ γ2	^{151}**C**	Q	L	Q	**L**	H	N	**F**	**P**	M	**D**	E	H	S	**C**^{165}
$5\text{-}HT_{3A}$	^{136}**C**	S	L	D	**I**	Y	N	**F**	**P**	F	**D**	V	Q	N	**C**^{150}
nACh α1	^{128}**C**	E	I	I	**V**	T	H	**F**	**P**	F	**D**	Q	Q	N	**C**^{142}

FIGURE 1: Amino acid alignment of the Cys loop of human GlyR α1, α2, α3, and *β*; $GABA_A$ α1, *β*2, and *γ*2; $5\text{-}HT_{3A}$; and *Torpedo* nACh α1 subunits. The bold type highlights the position of key functional residues.

Molecular Modeling. A molecular model of the GlyR α1 subunit was constructed using the PDB coordinates of the acetylcholine-binding protein (AChBP) (*19*) as a template for the extracellular domain of the protein and the PDB coordinates of a four-helical bundle found in bovine cytochrome *c* oxidase (1OCC) (*20*) as a template for the helices comprising the transmembrane domain (*21*−*24*). The primary sequence of the human GlyR α1 was edited to make a transmembrane domain sequence beginning at Tyr225 and ending at Arg414. The four predicted α-helical segments of GlyR were threaded separately onto the corresponding α-helical segments in the template of a four-helical bundle. Therefore, the edited sequence of GlyR was divided into four predicted α-helical segments: Ile225-Asn245, Ala251-Ser273, Ala282-Asn305, and Lys389-Arg414. These segments were aligned with the four α-helical segments in 1OCC, C129−C149, C161−C183, C195−C218, and C235−C258. We then generated the three interconnecting loops using the Homology module of Insight II (version 2000.1, Accelrys, San Diego, CA). The resulting model of the TMD corresponds closely to the coordinates in the homologous nAChR (1OED) (*13*). In the extracellular domain, we built loops to fill in gaps between the GlyR α1 sequence and the AChBP template sequence and refined the side chains in the model using the autorotamer feature in the Biopolymer Module of Insight II. The backbone atoms (C, Cα, and N) of each GlyR residue were tethered to the coordinates of the corresponding residues in the template with a force constant of 100 kcal/Å^2, and the structure was optimized with the Discover_3 module of Insight II to a derivative of 1 kcal/Å. Coulombic interactions were calculated with a constant dielectric of 1 and a cutoff at 9.5 Å. The structure was relaxed by performing 5000 2-fs steps of molecular dynamics at 298 K and was then reoptimized with Discover_3.

RESULTS

The Cys loop in the GlyR α1 subunit is defined by a disulfide bond that cross-links cysteine residues C138 and C152 (Figure 1). Each of the 13 amino acid residues within the Cys loop was individually mutated to alanine, and homomeric wild-type or mutant GlyRs were transiently

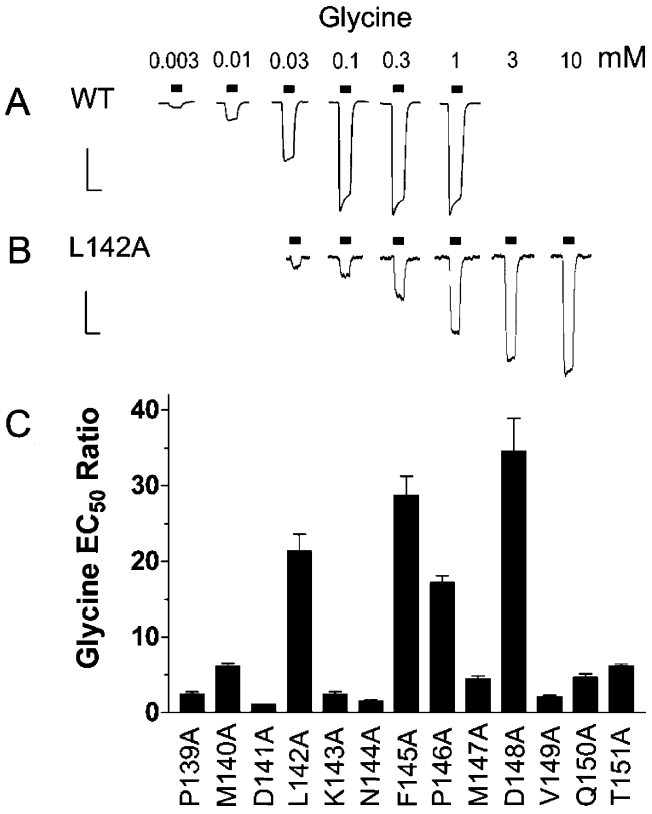

FIGURE 2: Representative electrophysiological recordings of glycine responses from HEK293 cells expressing the (A) wild-type and (B) mutated receptor L142A GlyR α1 homomers. (C) Effect of alanine mutations in the GlyR α1 subunit on agonist reponse. The glycine EC_{50} ratio is calculated as the mutant EC_{50} value divided by the wild-type EC_{50} value and is a measure of the change in glycine potency, with larger values corresponding to defects in receptor activation.

expressed in HEK293 cells. Inward Cl^- currents were evoked in a concentration-dependent manner by glycine (0.001−30 mM); representative current traces are shown in Figure 2A. All mutant receptors were expressed successfully and maximal current amplitudes were between 20 and 130% of that observed in the wild-type GlyR (data are summarized in Table 1). In seven of the mutated receptors, activation by glycine was little altered; in P139A, D141A, K143A, N144A, V149A, Q150A, and T151A, the glycine EC_{50} values, Hill coefficients, and maximal current amplitudes were not significantly different from the wild-type GlyR. The most deleterious mutations studied were L142A (Figure 2B), F145A, and P146A. The functional properties of these mutations were similar to those previously reported for alanine mutation at residue D148 (*15*); these receptors displayed large, ∼15−30-fold increases in the glycine EC_{50} and decreases in the Hill coefficient and maximal current. The mutant M140A displayed a significant decrease in glycine potency, with an increase in EC_{50}, from 27 ± 1 to 165 ± 15 μM ($p < 0.05$); the Hill slope value and maximal current were similar to those of the wild type. Alanine substitution at position M147 did not affect glycine potency but did significantly lower the Hill coefficient and maximal current. The effects of alanine substitution on GlyR activation are summarized in Figure 2C.

To further characterize the effects of alanine mutation, we examined receptor activation by the agonist taurine at wild-type and mutant GlyRs (Figure 3). Taurine displayed full

Table 1: Summary of Glycine Responses at Wild-Type and Mutant GlyRs[a]

	glycine activation			
GlyR α1	EC_{50} (μM)	n_H	I_{max} (pA)	*N*
wild type	27 ± 1	1.66 ± 0.06	−944 ± 77	26
P139A	67 ± 7	1.62 ± 0.14	−840 ± 81	13
M140A	165 ± 11[b]	1.08 ± 0.05[c]	−932 ± 71	12
D141A	29 ± 2	1.69 ± 0.12	−1228 ± 197	11
L142A	575 ± 61[c]	0.77 ± 0.03[c]	−291 ± 29[c]	14
K143A	66 ± 8	1.55 ± 0.10	−1157 ± 178	11
N144A	41 ± 5	1.69 ± 0.15	−948 ± 94	10
F145A	775 ± 69[c]	0.73 ± 0.02[c]	−250 ± 16[c]	10
P146A	463 ± 26[c]	0.86 ± 0.04[c]	−339 ± 44[c]	10
M147A	102 ± 12	1.33 ± 0.09[b]	−489 ± 60[c]	15
D148A[d]	932 ± 118[c]	0.82 ± 0.03[c]	−217 ± 19[c]	12
V149A	58 ± 4	1.87 ± 0.11	−1014 ± 91	11
Q150A	73 ± 10	1.71 ± 0.09	−1050 ± 125	13
T151A	145 ± 10	1.81 ± 0.07	−902 ± 113	11

[a] EC_{50} concentration, Hill coefficient (n_H), and maximal current (I_{max}) are presented as mean ± SE for *N* cells determined. Statistical significance from the wild type was assessed using a one-way ANOVA with Dunnett's multiple comparison post test. [b] $p < 0.05$. [c] $p < 0.01$. [d] Data reproduced from Schofield et al. (*15*).

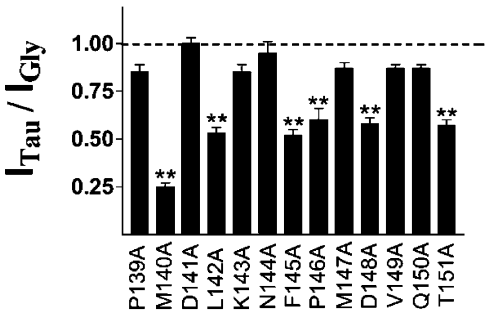

FIGURE 3: Effect of alanine mutation on GlyR activation by taurine. I_{Tau}/I_{Gly} represents the mean fraction of saturating glycine-gated current activated by 100 mM taurine. The dashed line marks the level of full efficacy displayed at the wild-type receptor. Values represent the mean of multiple cells ($n = 6-10$). Statistical significance from wild-type was assessed using one-way ANOVA with Dunnett's post test. The double asterisks indicate $p < 0.01$.

agonist action at the wild-type receptor ($EC_{50} = 100 \pm 5$ μM, $n_H = 1.47 \pm 0.06$, $\epsilon = 0.98 \pm 0.02$, and $n = 10$). In the mutant receptors P139A, D141A, K143A, N144A, M147A, V149A, and Q150A, the mean fraction of saturating glycine-gated current activated by 100 mM taurine (I_{Tau}/I_{Gly}) was from 0.85 to 1.00. In contrast, taurine sensitivity was significantly reduced at the mutants L142A ($I_{Tau}/I_{Gly} = 0.53 \pm 0.03$, $n = 7$), F145A ($I_{Tau}/I_{Gly} = 0.52 \pm 0.03$, $n = 7$), P146A ($I_{Tau}/I_{Gly} = 0.60 \pm 0.06$, $n = 6$), and D148A ($I_{Tau}/I_{Gly} = 0.58 \pm 0.03$, $n = 8$). The mutant T151A displayed a significant decrease in the potency of taurine ($EC_{50} = 2.26 \pm 0.22$ mM, $n_H = 0.85 \pm 0.08$, $I_{Tau}/I_{Gly} = 0.57 \pm 0.03$, and $n = 7$). The largest reduction in taurine sensitivity was observed at M140A ($I_{Tau}/I_{Gly} = 0.25 \pm 0.02$, $n = 8$).

To investigate the involvement of Cys loop residues in the allosteric modulation of the GlyR, we then studied submaximal agonist responses at wild-type and mutant receptors in the presence of halothane or isoflurane. Glycine EC_{20} concentrations were first calculated for the wild-type and each individual mutated receptor, using the data from Table 1. Each receptor was then activated with the appropriate EC_{20} concentration of glycine, and then halothane or isoflurane was preapplied for 3 s before a coapplication of

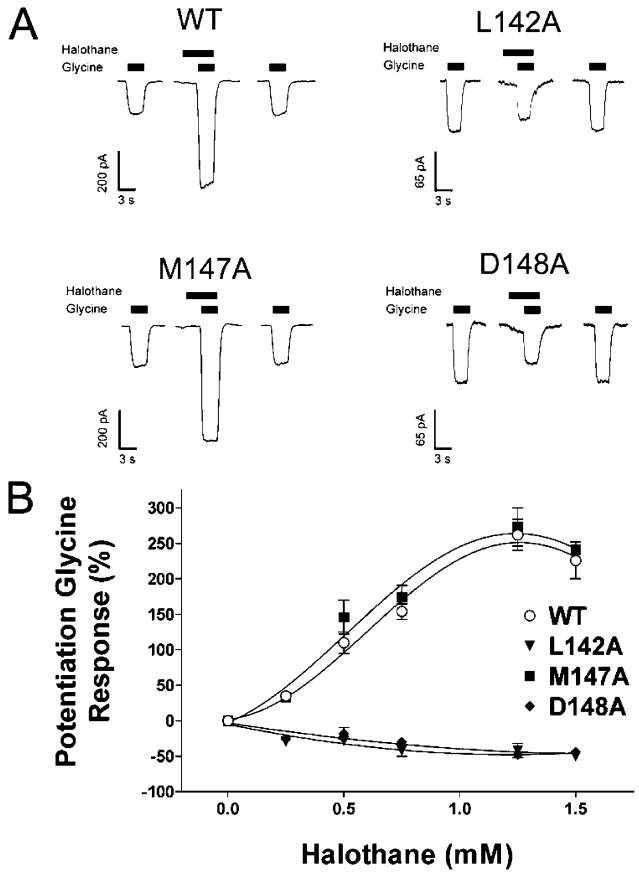

FIGURE 4: Action of halothane at wild-type and mutant GlyRs. (A) Representative electrophysiological recordings from HEK293 cells expressing the wild type and mutants, M147A, L142A, and D148A, GlyR α1 homomers. Cl^- currents were evoked by a 3 s application of each receptor's calculated EC_{20} concentration of glycine (first and third traces). Halothane was preapplied for 3 s before coapplication of the EC_{20} concentration of glycine (middle traces). (B) Halothane concentration−response curves for the wild type and GlyR mutants M147A, L142A, and D148A. Each data point represents the mean of multiple cells ($n = 5-11$).

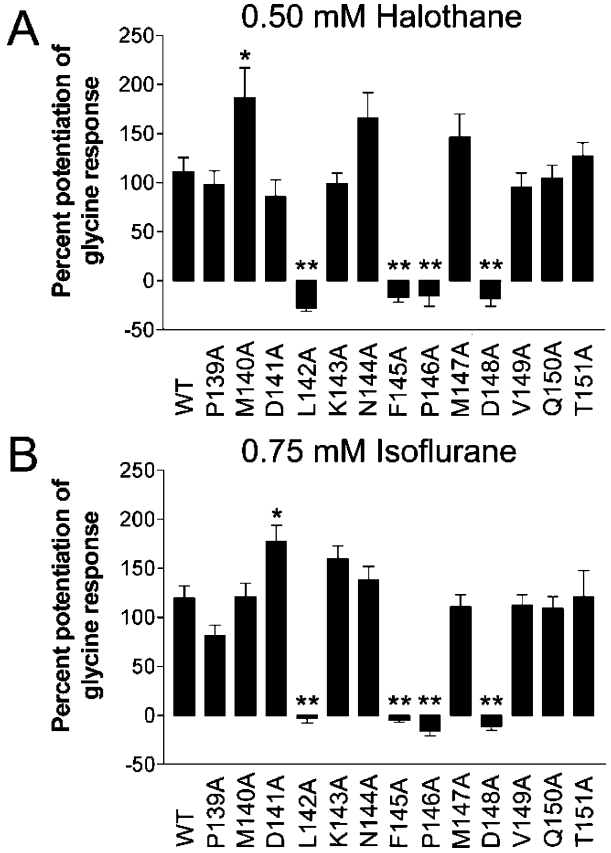

FIGURE 5: Effect of alanine mutations in the GlyR α1 subunit on submaximal agonist modulation by (A) 0.50 mM halothane and (B) 0.75 mM isoflurane. Values represent the mean of multiple cells ($n = 5-13$). Statistical significance from the wild type was assessed using one-way ANOVA with Dunnett's post test. The single asterisks indicate $p < 0.05$, and the double asterisks indicate $p < 0.01$.

glycine, followed by removal of the anesthetic and a third (recovery) application of glycine (Figure 4A). Halothane and isoflurane were applied within the range of clinically relevant concentrations (*25*). Wild-type receptors showed robust potentiation of the glycine response by 0.50 mM halothane (110 ± 15%, $n = 10$) and 0.75 mM isoflurane (120 ± 15%, $n = 13$). Seven of the mutant receptors, P139A, K143A, N144A, M147A, V149A, Q150A, and T151A, displayed normal sensitivity to halothane and isoflurane (potentiation ranging from 81 ± 11 to 146 ± 24%). The mutated receptors M140A and D141A (parts A and B of Figure 5) showed a significant increase in their responses to halothane and isoflurane, respectively ($p < 0.05$). In contrast, the potentiating effects of isoflurane and halothane were completely abolished by the mutations L142A, F145A, P146A, and D148A (Figure 4A, and parts A and B of Figure 5), in some case revealing a small inhibitory effect of the anesthetic (Figure 4A). We constructed concentration-effect curves for halothane, which showed a concentration-dependent and saturable-enhancing effect of halothane in the wild-type GlyR, as well as in the mutant M147A. In contrast, mutation at residues L142 or D148 produced a loss of sensitivity to halothane across a wide range of anesthetic concentrations (Figure 4B).

To examine the effects of tryptophan substitution, we generated the additional mutant L142W. When expressed in HEK293 cells, this receptor displayed a normal glycine sensitivity ($EC_{50} = 22 \pm 2\ \mu M$, $n = 9$), a Hill slope ($n_H = 1.81 \pm 0.11$), maximal currents ($I_{max} = -988 \pm 174$), taurine potency ($EC_{50} = 66 \pm 5\ \mu M$, $n_H = 1.30 \pm 0.07$, $n = 8$), and taurine relative efficacy ($\epsilon = 0.93 \pm 0.04$, $n = 11$). We also measured potentiation by isoflurane and halothane at L142W. Both anesthetics potentiated submaximal glycine responses in the normal manner (halothane = 105 ± 11%, $n = 6$; isoflurane = 114 ± 15%, $n = 7$).

DISCUSSION

The present study outlines a role for the signature disulfide loop of the GlyR α1 subunit in the process of receptor activation. We have identified critical residues at positions L142, F145, and P146, which along with D148 (*15*) are required for optimal agonist response at the glycine receptor. The effects of alanine substitution in the Cys loop were position-specific, because mutation of residues adjacent to the critical residues produced little or no change in the receptor function. These four critical residues are highly conserved throughout the LGIC subunit family (Figure 1). For example, P146 and D148 are invariant in all LGIC subunits, while residue F145 is conserved as an aromatic residue, with a tyrosine residue present at the corresponding position in the $GABA_A$ β2 subunit.

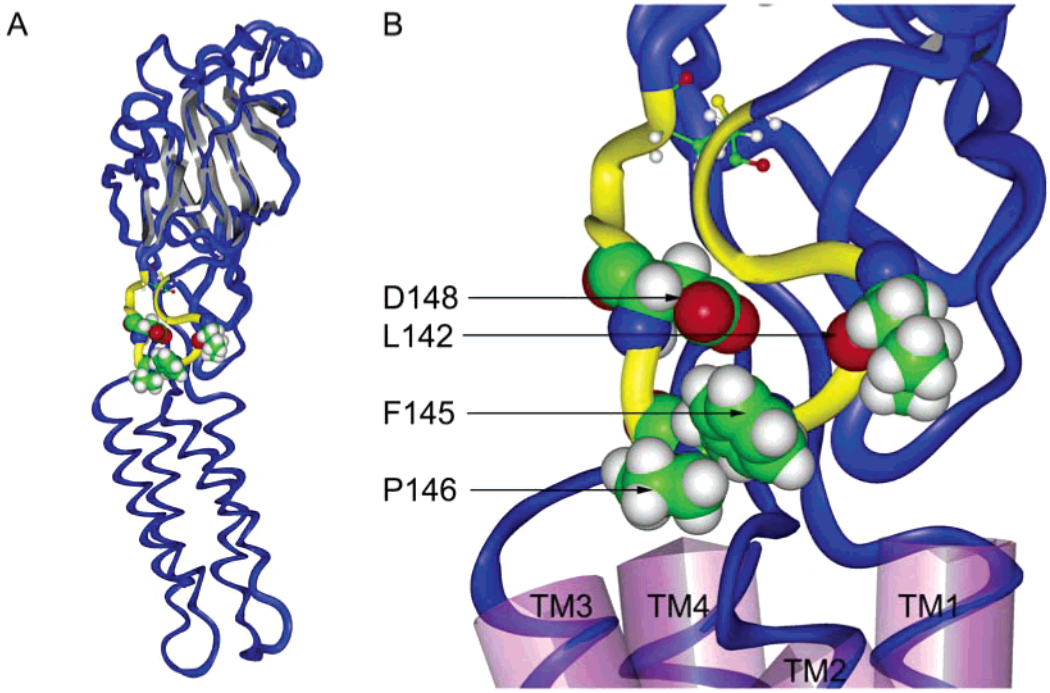

FIGURE 6: (A) Molecular model of the GlyR α1 subunit. The amino acid backbone is shown as a blue tube and the β strands, as gray ribbons. (B) View from the center of the ion channel, in the plane of the extracellular membrane surface. The Cys loop is highlighted yellow, and the four transmembrane α helices are shown as purple cylinders. The disulfide bond between C138 and C152 is rendered in ball-and-stick format. Key residues identified in this study are rendered with space-filling surfaces to show their position; carbon, nitrogen, oxygen, and hydrogen atoms are colored green, blue, red, and white, respectively.

Several pieces of evidence support the suggestion that the Cys loop is involved in receptor activation but not in agonist binding. First, previous work suggests that mutation of the highly conserved GlyR α1 residue D148 alters channel gating and not agonist binding (*15*, *26*). Second, mutation at residues L142, F145, and P146 all produced receptors with increases in the glycine EC_{50}, decreases in the Hill slope, lower maximal currents, and decreased sensitivity to taurine; all of these changes are highly characteristic of defects in the channel-gating mechanism (*27*, *28*). Third, molecular modeling of the GlyR based on the AChBP structure, showed that the agonist binding site is located approximately 30 Å from the critical residues of the Cys loop (Figure 6), and this distance was confirmed recently in a structure derived from cryo-electron microscopy images of the nAChR (*13*). This relatively large separation suggests that mutation in the Cys loop is unlikely to alter agonist binding, *unless* it causes a significant and widespread conformational change in the protein.

There is a limited degree of variability among the amino acids homologous with GlyR α1(L142). While leucine is conserved in all GlyR and $GABA_A$ subunits, the corresponding residue in the $5\text{-}HT_3$ receptor is an isoleucine and in the nAChR subunits, a valine. Single channel analysis of the mutation nAChRα(V132L), which is linked to a form of congenital myasthenic syndrome (*29*), showed a defect in receptor function, and this was attributed to a decrease in agonist-binding affinity. It was hypothesized that the mutation nAChRα(V132L) alters the distant agonist-binding site because of the displacement of the adjacent β strand, as a consequence of the incorporation of a larger side chain at this position. To determine whether this might also occur in the GlyR, we mutated the homologous residue L142 to tryptophan, which increases the molecular volume at this position by approximately 63.8 $Å^3$, and studied the function of the mutant receptor GlyR α1(L142W). This receptor displayed normal glycine sensitivity, maximal currents, and taurine efficacy. Our experimental results with L142A and L142W are clearly not consistent with a large-scale conformational change in the GlyR α1 subunit protein elicited by alanine (or tryptophan) mutagenesis. The apparent discrepancy between these and previous experimental results in the nAChR may reflect a degree of functional divergence in the role of the Cys loop among LGIC family members.

The ablation of positive allosteric modulation by halothane or isoflurane in the mutant receptors L142A, F145A, P146A, or D148A indicates that the Cys loop is important for the action of these compounds. Two possible explanations for these observed effects are (1) the Cys loop may form part of a binding pocket within which volatile anesthetics act or (2) the Cys loop participates in a conformational change that is necessary for receptor modulation by the inhaled anesthetics. Our data indicate that the first mechanism is unlikely. If the Cys loop is forming part of the anesthetic binding pocket, then substitution of one of these critical residues with a larger side chain would be expected to prevent the binding of halothane or isoflurane and fully or partially block potentiation. This method has been used previously to delineate the anesthetic binding cavity in the GlyR α1 subunit located between TM2 and TM3 formed by residues S267 and A288 (*30*). To test this idea, we measured potentiation by isoflurane and halothane at the mutant receptor GlyR α1(L142W). Both anesthetics potentiated submaximal glycine responses in the normal manner. The experiments with L142A and L142W seem consistent with the idea that volatile anesthetics are not directly binding to the Cys loop but that critical residues within the Cys loop are required for the receptor to undergo the conformational

changes necessary for the potentiation of agonist activation by the anesthetic. Additionally, we found that the mutations M140A and D141A produced increases in response to halothane and isoflurane, respectively. One possible explanation is that if the Cys loop is indeed mobile during channel gating, as suggested for the $GABA_A$ receptor (*16*), then a decreased steric interference caused by substituting alanine for larger residues at certain positions might perhaps promote gating and the modulation of gating by anesthetics.

A molecular model of the GlyR α1 subunit shows that the Cys loop is positioned in a region of the receptor at the interface between the extracellular and transmembrane domains (Figure 6). Interestingly, two of the four critical residues identified in the GlyR (L142 and F145) have amino acid side chains that are very hydrophobic, and these appear to be positioned along one face of the Cys loop, where they might form favorable interactions with other hydrophobic domains. The amphipathic nature of the Cys loop might allow it to move between hydrophilic and hydrophobic environments during receptor activation, as recently demonstrated in the nAChR (31).

The common genetic ancestry of LGIC subunits would imply that conserved residues within conserved structural domains of the receptor mediate important receptor functions that are similar among the LGIC family. The data presented here indicate that conserved residues in the Cys loop are critical for both optimal agonist-dependent activation and allosteric modulation by anesthetics in the GlyR.

REFERENCES

1. Langosch, D., Thomas, L., and Betz, H. (1988) Conserved quaternary structure of ligand-gated ion channels: The postsynaptic glycine receptor is a pentamer, *Proc. Natl. Acad. Sci. U.S.A. 85*, 7394−7398.
2. Ortells, M. O. (1997) Prediction of the secondary structure of the nicotinic acetylcholine receptor nontransmembrane regions, *Proteins 29*, 391−398.
3. Tang, P., Mandal, P. K., and Xu, Y. (2002) NMR structures of the second transmembrane domain of the human glycine receptor α(1) subunit: Model of pore architecture and channel gating, *Biophys. J. 83*, 252−262.
4. Vandenberg, R. J., Handford, C. A., and Schofield, P. R. (1992) Distinct agonist- and antagonist-binding sites on the glycine receptor, *Neuron 9*, 491−496.
5. Bormann, J., Rundstrom, N., Betz, H., and Langosch, D. (1993) Residues within transmembrane segment M2 determine chloride conductance of glycine receptor homo- and hetero-oligomers, *EMBO J. 12*, 3729−3737.
6. Griffon, N., Buttner, C., Nicke, A., Kuhse, J., Schmalzing, G., and Betz, H. (1999) Molecular determinants of glycine receptor subunit assembly, *EMBO J. 18*, 4711−4721.
7. Rajendra, S., Lynch, J. W., and Schofield, P. R. (1997) The glycine receptor, *Pharmacol. Ther. 73*, 121−146.
8. Breitinger, H. G., and Becker, C. M. (2002) The inhibitory glycine receptor-simple views of a complicated channel, *ChemBioChem 3*, 1042−1052.
9. Laube, B., Maksay, G., Schemm, R., and Betz, H. (2002) Modulation of glycine receptor function: A novel approach for therapeutic intervention at inhibitory synapses? *Trends Pharmacol. Sci. 23*, 519−527.
10. Zhang, Y., Laster, M. J., Hara, K., Harris, R. A., Eger, E. I., II, Stabernack, C. R., and Sonner, J. M. (2003) Glycine receptors mediate part of the immobility produced by inhaled anesthetics, *Anesth. Analg. 96*, 97−101.
11. Harrison, N. L., Kugler, J. L., Jones, M. V., Greenblatt, E. P., and Pritchett, D. B. (1993) Positive modulation of human γ-aminobutyric acid type A and glycine receptors by the inhalation anesthetic isoflurane, *Mol. Pharmacol. 44*, 628−632.
12. Mihic, S. J., Ye, Q., Wick, M. J., Koltchine, V. V., Krasowski, M. D., Finn, S. E., Mascia, M. P., Valenzuela, C. F., Hanson, K. K., Greenblatt, E. P., Harris, R. A., and Harrison, N. L. (1997) Sites of alcohol and volatile anaesthetic action on GABA(A) and glycine receptors, *Nature 389*, 385−389.
13. Miyazawa, A., Fujiyoshi, Y., and Unwin, N. (2003) Structure and gating mechanism of the acetylcholine receptor pore, *Nature 424*, 949−955.
14. Mascia, M. P., Trudell, J. R., and Harris, R. A. (2000) Specific binding sites for alcohols and anesthetics on ligand-gated ion channels. *Proc. Natl. Acad. Sci. U.S.A. 97*, 9305−9310.
15. Schofield, C. M., Jenkins, A., and Harrison, N. L. (2003) A highly conserved aspartic acid residue in the signature disulfide loop of the α1 subunit is a determinant of gating in the glycine receptor, *J. Biol. Chem. 278*, 34079−34083.
16. Kash, T. L., Jenkins, A., Kelley, J. C., Trudell, J. R., and Harrison, N. L. (2003) Coupling of agonist binding to channel gating in the GABA(A) receptor, *Nature 421*, 272−275.
17. Absalom, N. L., Lewis, T. M., Kaplan, W., Pierce, K. D., and Schofield, P. R. (2003) Role of charged residues in coupling ligand binding and channel activation in the extracellular domain of the glycine receptor, *J. Biol. Chem. 278*, 50151−50157.
18. Dougherty, D. A., and Lester, H. A. (2001) Neurobiology. Snails, synapses, and smokers, *Nature 411*, 252−253, 255.
19. Brejc, K., van Dijk, W. J., Klaassen, R. V., Schuurmans, M., van Der Oost, J., Smit, A. B., and Sixma, T. K. (2001) Crystal structure of an ACh-binding protein reveals the ligand-binding domain of nicotinic receptors, *Nature 411*, 269−276.
20. Tsukihara, T., Aoyama, H., Yamashita, E., Tomizaki, T., Yamaguchi, H., Shinzawa-Itoh, K., Nakashima, R., Yaono, R., and Yoshikawa, S. (1996) The whole structure of the 13-subunit oxidized cytochrome *c* oxidase at 2.8 Å, *Science 272*, 1136−1144.
21. Yamakura, T., Bertaccini, E., Trudell, J. R., and Harris, R. A. (2001) Anesthetics and ion channels: Molecular models and sites of action, *Annu. Rev. Pharmacol. Toxicol. 41*, 23−51.
22. Trudell, J. R., and Bertaccini, E. (2002) Molecular modelling of specific and non-specific anaesthetic interactions, *Br. J. Anaesth. 89*, 32−40.
23. Bertaccini, E., and Trudell, J. R. (2002) Predicting the transmembrane secondary structure of ligand-gated ion channels, *Protein Eng. 15*, 443−454.
24. Trudell, J. R., and Bertaccini, E. (2004) Comparative modeling of a GABAA α1 receptor using three crystal structures as templates, *J. Mol. Graphics Modell. 23*, 39−49.
25. Downie, D. L., Hall, A. C., Lieb, W. R., and Franks, N. P. (1996) Effects of inhalational general anaesthetics on native glycine receptors in rat medullary neurones and recombinant glycine receptors in *Xenopus* oocytes, *Br. J. Pharmacol. 118*, 493−502.
26. Vandenberg, R. J., Rajendra, S., French, C. R., Barry, P. H., and Schofield, P. R. (1993) The extracellular disulfide loop motif of the inhibitory glycine receptor does not form the agonist binding site, *Mol. Pharmacol. 44*, 198−203.
27. Lynch, J. W., Rajendra, S., Pierce, K. D., Handford, C. A., Barry, P. H., and Schofield, P. R. (1997) Identification of intracellular and extracellular domains mediating signal transduction in the inhibitory glycine receptor chloride channel, *EMBO J. 16*, 110−120.
28. Colquhoun, D. (1998) Binding, gating, affinity, and efficacy: The interpretation of structure−activity relationships for agonists and of the effects of mutating receptors, *Br. J. Pharmacol. 125*, 924−947.
29. Shen, X. M., Ohno, K., Tsujino, A., Brengman, J. M., Gingold, M., Sine, S. M., and Engel, A. G. (2003) Mutation causing severe myasthenia reveals functional asymmetry of AChR signature cystine loops in agonist binding and gating, *J. Clin. Invest. 111*, 497−505.
30. Wick, M. J., Mihic, S. J., Ueno, S., Mascia, M. P., Trudell, J. R., Brozowski, S. J., Ye, Q., Harrison, N. L., and Harris, R. A. (1998) Mutations of γ-aminobutyric acid and glycine receptors change alcohol cutoff: Evidence for an alcohol receptor? *Proc. Natl. Acad. Sci. U.S.A. 95*, 6504−6509.
31. Leite, J. F., Blanton, M. P., Shahgholi, M., Dougherty, D. A., and Lester, H. A. (2003) Conformation-dependent hydrophobic photolabeling of the nicotinic receptor: Electrophysiology-coordinated photochemistry and mass spectrometry, *Proc. Natl. Acad. Sci. U.S.A. 100*, 13054−13059.

BI036159G